# Superconducting and Semiconducting Magnetic Charge Transfer Salts: (BEDT-TTF)$_4$AFe($C_2O_4$)$_3$·$C_6H_5CN$ (A = $H_2O$, K, $NH_4$)

**Mohamedally Kurmoo,[†] Anthony W. Graham,[†] Peter Day,*[,†] Simon J. Coles,[‡] Michael B. Hursthouse,[‡] Jason L. Caulfield,[§] John Singleton,[§] Francis L. Pratt,[§] William Hayes,[§] Laurent Ducasse,[⊥] and Philippe Guionneau[⊥]**

*Contribution from the Davy Faraday Research Laboratory, Royal Institution of Great Britain, 21 Albemarle Street, London W1X 4BS, U.K., School of Chemistry and Applied Chemistry, University College of Wales, Cardiff CF1 3TB, U.K., Clarendon Laboratory, Parks Road, Oxford OX1 3PU, U.K., and Université Bordeaux I, 351 cours de la Liberation, Talence 33405, France*

*Received July 17, 1995*[⊗]

**Abstract:** Three new molecular charge transfer salts of bis(ethylenedithio)tetrathiafulvalene (BEDT-TTF), (BEDT-TTF)$_4$AFe($C_2O_4$)$_3C_6H_5CN$ (A = $H_2O$, K, $NH_4$), have been prepared, and their crystal structures and physical properties determined. The structures of all three salts consist of successive layers of BEDT-TTF and layers of approximately hexagonal geometry containing alternating A and Fe($C_2O_4$)$_3^{3-}$, with $C_6H_5CN$ lying within the hexagonal cavities. When A = K or $NH_4$ the BEDT-TTF layers consist of dimers (BEDT-TTF)$_2^{2+}$ separated by isolated (BEDT-TTF)$^0$, the charge difference being estimated from the C=C and C−S bond lengths. These salts are semiconductors ($\sigma \sim 10^{-4}$ S cm$^{-1}$, $E_A$ = 0.14 eV), and their magnetic susceptibilities are dominated by $S = {}^5/_2$Fe$^{III}$. The EPR spectra accordingly show only one sharp signal. When A = $H_2O$ the BEDT-TTF adopt the $\beta''$ packing, and the salt is a superconductor ($T_c$ 7.0(3) K). The magnetic susceptibility above the critical temperature is the sum of a Pauli component ($2 \times 10^{-3}$ emu mol$^{-1}$) and a Curie−Weiss term. Below the transition the susceptibility depends on the field penetration according to the London penetration depth, increasing with increasing field until the critical field. The Meissner effect is almost complete, indicating absence of pinning. The EPR spectra of the A = $H_2O$ compound are characterized by two resonances, one of Dysonian shape due to the conduction electrons on the organic cations and the other of Lorentzian shape arising from the 3d electrons of Fe$^{III}$. Electronic band structure calculations suggest that the A = K compound is semiconducting ($E_g$ = 0.3 eV) in good agreement with that result obtained from electrical measurement and the A = $H_2O$ is metallic ($W$ = 1.1 eV) with both electron and hole pockets in the Fermi surface. Optical reflectivity of the latter gives an electronic bandwidth of 1.0 eV, fully consistent with the band structure calculation.

## Introduction

A challenge in synthesizing new molecular-based materials is to bring together in the same crystal lattice combinations of physical properties that are not normally found in chemically simpler continuous lattice compounds. A feature of the superconducting charge transfer salts based on the donor molecule bis(ethylenedithio)tetrathiafulvalene (BEDT-TTF) is the spatial segregation of the organic cations and inorganic anions into alternating layers, which has led us to cite them as examples of "organic−inorganic molecular composites" [1] or "chemically constructed multilayers".[2] Because of this separation into well-defined organic and inorganic components the BEDT-TTF charge transfer salts appear attractive synthetic targets for attempts to combine superconductivity in a molecular lattice with properties more characteristic of the inorganic solid state like cooperative magnetism. The electrons close to the Fermi surface are largely confined to frontier orbitals of the BEDT-TTF, while magnetic moments localized on the anions can be built in if the latter are transition metal complexes.

Establishing superconductivity in a crystal lattice containing localized magnetic moments is a desirable aim because superconductivity and magnetism have long been considered inimical to one another: Cooper pairs are disrupted both by externally applied fields or by the internal fields generated in ferromagnets.[3] Nevertheless a few examples exist of magnetic superconductors containing 4f elements (Ln) such as the Chevrel phases $LnMo_6S_8$,[4] the borides $LnRh_4B_4$,[5] and the cuprates $LnBa_2Cu_3O_7$.[6] No corresponding stoichiometric phases containing 3d ions have been reported. Of the small number of BEDT-TTF salts containing 3d complex anions, several are semiconductors,[7] but we reported one example, (BEDT-TTF)$_3CuCl_4$·$H_2O$, which remains metallic down to 400 mK though without becoming superconducting and in which magnetic resonance from the conduction electrons and the localized 3d electrons can be resolved.[8]

[†] Royal Institution.
[‡] University College of Wales.
[§] Clarendon Laboratory.
[⊥] Université Bordeaux.
[⊗] Abstract published in *Advance ACS Abstracts,* December 1, 1995.
(1) Day, P. *Philos. Trans. R. Soc. London* **1985**, *A314*, 145−158.
(2) Day, P. *Phys. Scr.* **1993**, *T49*, 726−730.
(3) See, e.g.: *Topics in Current Physics*; Fisher, Ø., Maple, M. B., Eds.; Springer Verlag: New York, 1983; Vols. 32, 34 passim.
(4) (a) Ishikawa, M.; Fischer, Ø. *Solid State Commun.* **1977**, *23*, 37. (b) Lynn, J. W.; Shirane, G.; Thomlinson, W.; Sheldon, R. N. *Phys. Rev. Lett.* **1981**, *46*, 368−371.
(5) (a) Fertig, W. A.; Johnston, D. C.; DeLong, L. E.; McCallum, R. W.; Maple, M. B.; Matthias, B. T. *Phys. Rev. Lett.* **1977**, *38*, 987−990. (b) Moncton, D. E.; McWhann, D. B.; Schmidt, P. H.; Shirane, G.; Thomlinson, W.; Maple, M. B.; MacKay, H. B.; Woolf, L. D.; Fisk, Z.; Johnston, D. C. *Phys. Rev. Lett.* **1980**, *45*, 2060−2063.
(6) Beauchamp, K. M.; Spalding, G. C.; Huber, W. H.; Goldman, A. M. *Phys. Rev. Lett.* **1994**, *73*, 2752−2755.
(7) (a) Mallah, T.; Hollis, C.; Bott, S.; Kurmoo, M.; Day, P. *J. Chem. Soc., Dalton Trans.* **1990**, 859−865. (b) Marsden, I. R.; Allan, M. L.; Friend, R. H.; Kurmoo, M.; Kanazawa, D.; Day, P.; Bravic, G.; Chasseau, D.; Ducasse, L.; Hayes, W. *Phys. Rev. B* **1994**, *50*, 2118−2127.
(8) Day, P.; Kurmoo, M.; Mallah, T.; Marsden, I. R.; Allan, M. L.; Friend, R. H.; Pratt, F. L.; Hayes, W.; Chasseau, D.; Bravic, G.; Ducasse, L. *J. Am. Chem. Soc.* **1992**, *114*, 10722−10729.

0002-7863/95/1517-12209$09.00/0 

**Table 1.** Crystal Data and Structure Refinement Data for $(BEDT\text{-}TTF)_4AFe(C_2O_4)_3\cdot C_6H_5CN$: (a) A = K, (b) A = $NH_4$, (c) A = $H_2O$

| | (a) | (b) | (c) |
|---|---|---|---|
| empirical formula | $C_{53}H_{37}FeKNO_{12}S_{32}$ | $C_{53}H_{41}FeN_2O_{12}S_{32}$ | $C_{53}H_{39}FeNO_{13}S_{32}$ |
| formula weight | 1999.70 | 1974.61 | 1979.78 |
| temperature | 120(2) K | 120(2) K | 120(2) K |
| wavelength | 0.71069 Å | 0.71069 Å | 0.71069 Å |
| crystal system | orthorhombic | orthorhombic | monoclinic |
| space group | *Pbcn* | *Pbcn* | *C2/c* |
| unit cell dimensions | $a = 10.33(2)$ Å | $a = 10.370(5)$ Å | $a = 10.232(12)$ Å |
| | $b = 19.53(3)$ Å | $b = 19.588(12)$ Å | $b = 20.04(3)$ Å |
| | $c = 35.94(2)$ Å | $c = 35.790(8)$ Å | $c = 34.97(2)$ Å |
| | | | $\beta = 93.25(11)$ deg |
| volume | 7252(15) Å$^3$ | 7270(6) Å$^3$ | 7157(13) Å$^3$ |
| Z | 4 | 4 | 4 |
| density (calculated) | 1.832 Mg/m$^3$ | 1.804 Mg/m$^3$ | 1.835 Mg/m$^3$ |
| absorption coefficient | 1.247 mm$^{-1}$ | 1.187 mm$^{-1}$ | 1.207 mm$^{-1}$ |
| $F(000)$ | 4056 | 4008 | 4016 |
| crystal size | 0.15 × 0.2 × 0.2 mm | | 0.2 × 0.2 × 0.07 mm |
| $\theta$ range for data collection | 2.09−25.07° | 2.08−25.07° | 2.33−24.87° |
| index ranges | $-10\le h\le 11$, $-15\le k\le 15$, $-39\le l\le 23$ | $-11\le h\le 11$, $-22\le k\le 22$, $-39\le l\le 8$ | $-8\le h\le 11$, $-22\le k\le 20$, $-39\le l\le 38$ |
| reflcns collected | 16763 | 14915 | 13774 |
| independent reflcns | 4796 [$R$(int) = 0.0562] | 5561 [$R$(int) = 0.0987] | 5110 [$R$(int) = 0.1011] |
| refinement method | full-matrix least-squares on $F^2$ | full-matrix least-squares on $F^2$ | full-matrix least-squares on $F^2$ |
| data; restraints; parameters | 4786; 0; 462 | 5561; 0; 205 | 5094; 6; 454 |
| goodness-of-fit on $F^2$ | 1.062 | 2.178 | 0.661 |
| final $R$ indices [$I > 2\sigma(I)$] | $R_1 = 0.0490$, $wR_2 = 0.1280$ | $R_1 = 0.1557$, $wR_2 = 0.3831$ | $R_1 = 0.0416$, $wR_2 = 0.0760$ |
| $R$ indices (all data) | $R_1 = 0.0596$, $wR_2 = 0.1416$ | $R_1 = 0.1902$, $wR_2 = 0.3935$ | $R_1 = 0.0982$, $wR_2 = 0.0934$ |
| largest diff. peak and hole | 0.702 and −1.185 e.Å$^{-3}$ | 2.371 and −1.516 e.Å$^{-3}$ | 0.651 and −0.439 e.Å$^{-3}$ |

Recently a number of instances have come to light of two-dimensional bimetallic layers containing uni- or dipositive cations and $M^{III}(C_2O_4)_3^{3-}$ in which the oxalato-ion acts as bridging ligand, leading to infinite sheets of approximately hexagonal symmetry, separated by bulky organic cations.[9,10] When the latter are electronically inactive the resulting compounds show interesting and unusual ferrimagnetic behavior.[11,12] In parallel with our studies of their magnetic properties we have therefore begun to explore the synthesis of compounds containing anion lattices of similar type but interleaved with BEDT-TTF molecules. The present paper reports the synthesis and crystal structures of three such compounds, $(BEDT\text{-}TTF)_4AFe(C_2O_4)_3\cdot C_6H_5CN$, (A = $H_2O$, K, $NH_4$) together with characterization of their physical properties. While the stoichiometric ratio of BEDT-TTF to Fe is the same in all three compounds, as is the basic topology of the anion layer, the presence or absence of a monopositive cation within the latter not only changes the electron count (and hence the band filling) in the organic layer but also drastically alters the packing motif of the BEDT-TTF. Thus, the compounds with A = K, $NH_4$ are semiconductors with the organic molecules present as $(BEDT\text{-}TTF)_2^{2+}$ and $(BEDT\text{-}TTF)^0$. In contrast the compound with A = $H_2O$ has BEDT-TTF packed in the $\beta''$ arrangement[13] and is the first example of a molecular superconductor containing magnetic ions. A preliminary account of part of this work has appeared.[14]

## Experimental Section

**Preparation.** BEDT-TTF was synthesized following the method of Larsen and Lenoir[15] and recrystallized from $CHCl_3$. $A_3Fe(C_2O_4)_3\cdot H_2O$ (A = K, $NH_4$) were prepared by literature methods[16] and recrystallized from water. $C_6H_5CN$ was dried over $CaCl_2$ and freshly distilled prior to use. 18-Crown-6-ether (Aldrich) was recrystallized from acetonitrile and dried in a dessiccator over $P_2O_5$. To remove small traces of $Fe(II)C_2O_4\cdot{}^3/_2H_2O$, the benzonitrile solution of the anion and the 18C6 was filtered before electrocrystallization.

Electrochemical crystal growth was carried out in conventional H-shaped cells with Pt electrodes in a constant temperature (295(2) K) over 20 days at a current of 1 $\mu$A. The cells were fixed inside sand-filled compartments on a concrete table to minimize vibration. Each cell contained 10 mg of BEDT-TTF and 100 mg of either $K_3Fe(C_2O_4)_3\cdot 3H_2O$ or $(NH_4)_3Fe(C_2O_4)_3\cdot 3H_2O$ together with 200 mg of 18-crown-6 in 50 mL of $C_6H_5CN$. Under dry conditions, for the K and $NH_4$ salts the crystals adhering to the anode were diamond shaped but upon addition of water to the cell with $(NH_4)_3Fe(C_2O_4)_3\cdot 3H_2O$ two phases were obtained, with diamond and needle morphology. The phases were identified from their crystal structures (see below) and by their morphology.

**Structure Determination.** The crystal structures of the three compounds with A = $H_2O$, K, $NH_4$ were determined from single crystal X-ray diffraction data collected at 120 K at University College of Wales, Cardiff, UK. The four circle diffractometer is equipped with a Delft Instruments FAST TV area detector and utilizes graphite monochromated Mo K$\alpha$ (0.71069 Å) radiation from a rotating anode generator.[17] Temperature was controlled by an Oxford Cryostream system. Lattice parameters ere initially derived from more than 50 reflections. Crystal data are tabulated in Table 1, with details of the refinements.

The structures were solved by direct methods using SHELXL 93[18] and refined by full-matrix least squares on $F^2$ for data corrected for Lorentz and polarization factors and also for absorption. The non-hydrogen atoms were refined with anisotropic temperature factors while the hydrogen atoms were refined freely with individual $U_{iso}$ values. The weighting scheme used was $w = 1/\sigma^2(F_0^2)$. Scattering factors were taken from the ref 18. The final reliability factors are given in Table 1.

(9) Tamaki, H.; Zhong, Z. J.; Matsumoto, N.; Kida, S.; Koikawa, M.; Achiwa, N.; Hashimoto, Y.; Okawa, H. *J. Am. Chem. Soc.* **1992**, *114*, 6974−6979.

(10) (a) Descurtins, S.; Schmalle, H. W.; Oswald, H. R.; Linden, A.; Ensling, J.; Gütlich, P.; Hauser, A. *Inorg. Chim. Acta* **1994**, *216*, 65−72. (b) Farrell, R. P.; Hambley, T. W.; Lay, P. *Inorg. Chem.* **1995**, *34*, 757−758.

(11) Mathonière, C.; Carling, S. G.; Dou, Y.; Day, P. *J. Chem. Soc., Chem. Commun.* **1994**, 1551−1552.

(12) Mathonière, C.; Nuttall, C. J.; Carling, S. G.; Day, P. *Inorg. Chem.* In press.

(13) Kurmoo, M.; Talham, D.; Day, P.; Parker, I. D.; Friend, R. H.; Stringer, A. M.; Howard, J. A. K. *Solid State Commun.* **1987**, *61*, 459−464.

(14) Graham, A. W.; Kurmoo, M.; Day, P. *J. Chem. Soc., Chem. Commun.* **1995**, 2061−2062.

(15) Larsen, J.; Lenoir, C. *Synthesis* **1988**, 2, 134.

(16) Bailar, J. C.; Jones, E. M. *Inorg. Synth.* **1939**, *1*, 35−39.

(17) Darr, J. A.; Drake, S. R.; Hursthouse, M. B.; Abdul Malik, K. M. *Inorg. Chem.* **1993**, *32*, 5704−5708.

(18) Sheldick, G. M. SHELXL 93 Programme System. *J. Appl. Crystallogr.* In press.

**Electronic Band Structure.** The electronic band structures of both the semiconducting A = K and superconducting A = $H_2O$ compounds were calculated in the tight binding approximation within the Extended Hückel hamiltonian using the highest filled molecular orbitals (HOMO) of BEDT-TTF as basis functions. Transfer integrals were calculated using the dimer splitting model.[19] For crystal structures containing several crystallographically independent molecules in the unit cell this approach allows us to determine the difference in the HOMO energies of the different molecules which are then taken into account in the band structure calculation. These differences may be crucial in evaluating the electronic gap in semiconducting salts when they become large compared to the bandwidth, as for example in $(TMTSF)_2ReO_4$ below the anion ordering temperature.[20] In the present series, the two BEDT-TTF in the A = K compound carry distinctly different charges and hence the respective HOMOs have different energies.

**Electrical Conductivity.** Two-probe dc and both four-probe ac (15−33 Hz) and dc resistance measurements were made on single crystals with current flow along different axes. Electrical contacts to the crystals were made with 25 $\mu$m gold wire and platinum paint. The crystals were held in an Oxford Instruments continuous flow helium cryostat, and temperature was monitored by a Rh−Fe sensor. Magnetoresistance measurements of the metallic salt were made in the same way but with the crystal holder placed within the superconducting solenoid of a Quantum Design MPMS 7 SQUID magnetometer. The temperature was swept from 2 to 7 K at different applied fields in the range 1−640 mT. The contacts were 4 in a line and the current applied was 10 $\mu$A. Contact resistances were ~30 Ω per pair and the nested/unnested voltage was >100.

**Magnetic Susceptibility.** Measurements were made on polycrystalline samples held in gelatine-capsules inside a plastic tube (drinking straw) using a Quantum Design MPMS 7 SQUID magnetometer. Magnetization data were taken in different applied fields on warming from 2 to 300 K. Correction was made to the measured susceptibility for core diamagnetism using Pascal constants. To detect a Meissner effect in the A = $H_2O$ compound the sample was cooled in zero field to 2 K prior to measuring the magnetization on warming to 10 K in a field of 5 G followed by cooling to 2 K in the same field. This procedure was followed for increasing field up to 410 G. To circumvent the remnent field of the superconducting solenoid the low field magnetization was measured as a function of applied field to locate the value of the applied field at which the magnetization was zero above the superconducting transition within the detection limit of the magnetometer.

**Electron Spin Resonance.** Electron spin resonance spectra of single crystals of the A = K and A = $H_2O$ compounds as well as a polycrystalline sample of $K_3Fe(C_2O_4)_3\cdot 3H_2O$ for comparison were measured at room temperature on a Varian E9 reflection spectrometer operating at 9.2 GHz. The crystals were oriented in a $TE_{102}$ cavity by means of a home made goniometer.

**Optical Reflectivity.** Spectra were recorded at room temperature on two instruments: a Perkin Elmer 1710 equipped with a Spectra Tech microscope and an evacuable Bruker 66VS employing a Specac reflection attachment. KRS5 was used as polarizer. All data were referenced to a gold mirror, and data from the Bruker spectrometer were then normalized to that of the absolute value obtained on the Perkin Elmer instrument. A flat needle crystal was glued onto two pieces of fine (100 $\mu$m) noninsulated copper wire and then suspended on a washer mount to minimize the effect of stray light. For measurements under the microscope the crystal was placed on a transparent KBr plate.

## Results and Discussion

**Crystal Structures.** The crystal structures of all three compounds consist of alternating layers containing only BEDT-TTF and only $AFe(C_2O_4)_3\cdot C_6H_5CN$. Whilst the molecular packing in the latter is quite similar in all three cases, the molecular packing arrangement within the BEDT-TTF layers differs markedly from the other two when A = $H_2O$. We therefore describe the anion layers together but consider the BEDT-TTF layers separately. Crystals of the $NH_4$ salt were invariably twinned so the structure determination in that case is much less precise. However, it is sufficient to delineate the broad outlines of the structure. Selected bond lengths and angles relevant to the anion layers and the central tetrathiafulvalene moieties of the BEDT-TTF are listed in Tables 2 and 3. Numbering of the atoms is given in Figure 1.

When projected on to the mean plane of the A and Fe, the anion layers have a clear honeycomb arrangement, with alternate A and Fe forming an approximately hexagonal network (Figure 2). The Fe are octahedrally coordinated by three bidentate oxalate ions, giving rise to a trigonal component of the crystal field. The mean Fe−O bond lengths (2.011 Å) are identical in the K and $H_2O$ compounds though the extent of the trigonal distortion is greater in the latter, as measured by the mean *trans* O−Fe−O angles (K, 170.6°; $H_2O$, 164.1°). In the discrete $Fe(C_2O_4)_3^{3-}$ as found in the $NH_4$ salt the corresponding figures are Fe−O 2.002 Å, *trans* O−Fe−O 163.5°.[21] The O atoms of the oxalate which are not coordinated to Fe form cavities occupied either by K or $H_2O$. In the former case the coordination number of the K is seven, since the CN group of a benzonitrile molecule is oriented toward it with the N−K distance being 2.952 Å (Figure 2a). The benzonitrile molecules show twofold disorder with respect to the orientation of the CN group but occupy cavities in the $KFe(C_2O_4)_3$ lattice of approximately hexagonal shape. The mean plane of the benzonitrile coincides with that found by the K and Fe, and there can be little doubt that it performs an important "templating" role in stabilizing the lattice. The mean K−O bond length of 2.87 Å is close to that expected.

Turning to the superconducting phase, the underlying hexagonal network of Fe and A is retained. A crystallographic point crucial to rationalizing the electronic structure and properties concerns the nature and disposition of the atoms occupying the cavity analogous to the one that contains K or $NH_4$ in the semiconducting phases. Attempts to refine a structure based on occupation by N failed, while assumption that the atom occupying the cavity was O proved successful (Table 1). Furthermore, the electron count (and hence the Fermi energy) depends on whether the species in question is $H_2O$ or $H_3O^+$. The H atoms could not be located, but two pieces of evidence point strongly to the molecular species being $H_2O$. First, the site symmetry of the O is $C_2$, and the distances to the six O on neighboring $C_2O_4^{2-}$ are 2.81 (×2), 2.93 (×2), 2.95 Å (×2), i.e., two distances are distinctly shorter than the other four. Second, the two closest oxalate O subtend an angle of 137.4° at the central O, quite compatible with a H-bonded $H_2O$. For example in $(COOD)_2\cdot 2D_2O$ the distances between the $D_2O$ and CO groups are 2.84−2.90 Å and the O−D···O angles are 156° and 168°.[22]

In the A = $H_2O$ compound the included benzonitrile molecules are fully ordered, with the −CN groups oriented toward Fe, so the hexagonal network of Fe and $H_2O$ is elongated along one axis. There is an accompanying lowering of symmetry from orthorhombic to monoclinic ($\beta$ = 93.2°), although the unit cell parameters and volumes of the K and $H_2O$ compounds are quite comparable (7252 and 7157 Å$^3$, respectively). It appears that in the K-salt the lattice is loosely packed probably as a result of the hexagonal structure forced on the BEDT-TTF layer by the Fe oxalate sublattice. The difference of ~100 Å$^3$ is equivalent to an extra 4−5 atoms.

A final structural point about the anion layers concerns their chirality. The point symmetry of $Fe(C_2O_4)_3^{3-}$ is $D_3$, and the

(19) Ducasse, L.; Abderrabba, A.; Hoarau, J.; Pesquer, M.; Gallois, B.; Gaultier, J. *J. Phys. C: Solid State Phys.* **1986**, *19*, 3805−3820.
(20) Ducasse, L.; Abderrabba, A.; Gallois, B.; Chasseau, D. *Synth. Met.* **1987**, *19*, 327−332.

**Table 2.** Selected Bond Lengths (Å) and Angles (deg) for $(BEDT\text{-}TTF)_4AFe(C_2O_4)_3\cdot C_6H_5CN$ (A = K, $NH_4$)

| | K | $NH_4$ | | K | $NH_4$ |
|---|---|---|---|---|---|
| Fe(1)−O(1) | 1.998(4) 2× | 1.997(10) | A(1)−O(5) | 2.825(6) | 2.91(2) |
| Fe(1)−O(3) | 2.019(4) 2× | 2.012(10) | A(1)−O(6) | 2.878(5) | 2.88(3) |
| Fe(1)−O(4) | 2.017(4) 2× | 1.999(11) | | | |
| O(1)−C(21) | 1.279(8) | 1.23(2) | O(4)−C(23) | 1.292(7) | 1.25(2) |
| O(2)−C(21) | 1.219(8) | 1.27(2) | O(5)−C(22) | 1.210(7) | 1.26(2) |
| O(3)−C(22) | 1.293(7) | 1.25(2) | O(6)−C(23) | 1.230(7) | 1.24(2) |
| C(22)−C(23) | 1.544(8) | 1.53(2) | C(21)−C(21)′ | 1.583(12) | 1.52(4) |
| | BEDT-TTF (1) | | | BEDT-TTF (2) | |
| S(3)−C(3) | 1.754(5) | 1.79(2) | S(11)−C(13) | 1.773(5) | 1.80(2) |
| S(3)−C(5) | 1.730(5) | 1.74(2) | S(11)−C(15) | 1.755(5) | 1.75(2) |
| S(4)−C(4) | 1.745(5) | 1.74(2) | S(12)−C(15) | 1.760(6) | 1.77(2) |
| S(4)−C(5) | 1.735(5) | 1.72(2) | S(12)−C(14) | 1.756(5) | 1.77(2) |
| S(4)−C(5) | 1.735(5) | 1.72(2) | S(12)−C(14) | 1.756(5) | 1.77(2) |
| S(5)−C(7) | 1.753(5) | 1.76(2) | S(13)−C(16) | 1.767(6) | 1.74(2) |
| S(5)−C(6) | 1.731(6) | 1.72(2) | S(13)−C(17) | 1.756(5) | 1.76(2) |
| S(6)−C(8) | 1.741(5) | 1.73(2) | S(14)−C(16) | 1.769(5) | 1.78(2) |
| S(6)−C(6) | 1.727(5) | 1.74(2) | S(14)−C(18) | 1.757(5) | 1.76(2) |
| C(3)−C(4) | 1.350(7) | 1.34(2) | C(13)−C(14) | 1.338(7) | 1.32(2) |
| C(5)−C(6) | 1.381(7) | 1.40(2) | C(15)−C(16) | 1.342(8) | 1.35(2) |
| C(7)−C(8) | 1.357(8) | 1.33(2) | C(17)−C(18) | 1.340(8) | 1.29(2) |
| C(9)−C(10) | 1.513(9) | 1.52(3) | | | |
| O(1)−Fe(1)−O(1)′ | 81.2(2) | 81.1(6) | C(21)−O(2)−K(1)″ | 120.7(4) | |
| O(4)−Fe(1)−O(3)′ | 91.8(2) 2× | 91.6(4) | C(21)−O(1)−Fe(1) | 116.0(4) | 113.4(11) |
| O(1)−Fe(1)−O(4) | 96.4(2) 2× | 96.7(4) | C(22)−O(5)−K(1) | 122.4(4) | |
| O(4)−Fe(1)−O(4)′ | 170.3(2) | 169.4(6) | C(22)−O(3)−Fe(1) | 114.5(3) | 113.4(10) |
| O(1)′−Fe(1)−O(4) | 91.0(2) 2× | 91.3(4) | C(23)−O(6)−K(1) | 119.9(4) | |
| O(4)−Fe(1)−O(3) | 81.3(2) 2× | 80.9(4) | C(23)−O(4)−Fe(1) | 114.1(3) | 114.3(10) |
| O(1)−Fe(1)−O(3) | 94.8(2) 2× | 94.7(4) | O(1)−Fe(1)−O(3)″ | 170.9(2) | 170.8(4) |
| O(3)′−Fe(1)−O(3) | 90.3(2) | 90.6(6) | | | |

**Table 3.** Selected Bond Lengths (Å) and Angles (deg) for $(BEDT\text{-}TTF)_4(H_2O)Fe(C_2O_4)_3\cdot C_6H_5CN$

| | | | |
|---|---|---|---|
| Fe(1)−O(1) | 2.008(3) | O(7)−O(3) | 2.95 |
| Fe(1)−O(2) | 2.011(3) | O(7)−O(4) | 2.81 |
| Fe(1)−O(5) | 2.016(3) | O(7)−O(6) | 2.93 |
| O(1)−C(21) | 1.292(5) | O(4)−C(22) | 1.235(5) |
| O(2)−C(22) | 1.285(5) | O(5)−C(23) | 1.268(5) |
| O(3)−C(21) | 1.221(5) | O(6)−C(23)′ | 1.243(5) |
| C(21)−C(22) | 1.549(6) | C(23)−C(23) | 1.536(9) |
| S(3)−C(5) | 1.744(4) | S(3)−C(3) | 1.752(4) |
| S(4)−C(5) | 1.749(4) | S(4)−C(4) | 1.768(4) |
| S(5)−C(6) | 1.739(5) | S(5)−C(7) | 1.764(4) |
| S(6)−C(8) | 1.732(4) | S(6)−C(6) | 1.755(4) |
| S(12)−C(14) | 1.739(4) | S(12)−C(15) | 1.756(4) |
| S(11)−C(15) | 1.741(4) | S(11)−C(13) | 1.750(4) |
| S(14)−C(16) | 1.732(5) | S(14)−C(18) | 1.766(5) |
| S(13)−C(16) | 1.746(4) | S(13)−C(17) | 1.747(5) |
| C(3)−C(4) | 1.343(5) | C(13)−C(14) | 1.351(6) |
| C(5)−C(6) | 1.345(6) | C(15)−C(16) | 1.363(6) |
| C(7)−C(8) | 1.369(6) | C(17)−C(18) | 1.335(6) |
| O(1)−Fe(1)−O(1)′ | 159.2(2) | O(2)′−Fe(1)−O(2) | 104.0(2) |
| O(1)−Fe(1)−O(2)′ | 86.77(13) | O(2)−Fe(1)−O(5) | 88.9(2) |
| O(1)−Fe(1)−O(2) | 80.46(13) | O(2)−Fe(1)−O(5)′ | 166.59(12) |
| O(1)−Fe(1)−O(5)′ | 96.88(12) | O(5)′−Fe(1)−O(5) | 78.5(2) |
| O(1)−Fe(1)−O(5) | 99.18(12) | | |

ion may exist in principle in Δ or Λ enantiomers. In the compounds reported in this paper, which were synthesized from racemic starting material, we find that alternate anion layers are composed exclusively either of Δ or Λ anions. It would be interesting to synthesize the corresponding salts with optically resolved anions. It is worth noting that an analogous sequence of Δ and Λ-containing layers is observed in the crystal structure of $P(C_6H_5)_4MnCr(C_2O_4)_3$ synthesized from racemic starting material.[10]

In contrast to the closely similar anion layers, the molecular arrangements in the BEDT-TTF layers are quite different in the K and $NH_4$ salts from that found in the $H_2O$ one. In the former the asymmetric unit consists of two independent BEDT-TTF, distinguished from one another in two ways. First, the terminal ethylene groups are staggered in one while being eclipsed in the other; second, the central C=C bond lengths differ markedly (1.340(8) and 1.381(7) Å). The latter difference signifies a difference in the charge states of the molecules. Comparison with corresponding bond lengths in other BEDT-TTF salts with established levels of oxidation[23] indicates charges of 0 and +1. The unipositive ions occur as face-to-face dimers, surrounded by monomeric neutral molecules (Figure 3a). Molecular planes of neighboring dimers along [011] are oriented nearly orthogonal to one another, as in the κ-phase structure of $(BEDT\text{-}TTF)_2X$,[24] but the planes of the dimers along [100] are parallel. Different charge states of BEDT-TTF have been found to coexist in the same lattice,[25] but the arrangement of $(BEDT\text{-}TTF)_2^{2+}$ surrounded by $(BEDT\text{-}TTF)^0$ has not been observed before. The distance between the mean plane of the molecules within the dimer (3.36 Å) is short, and the mode of overlap is not quite the "bond over ring" arrangement found in the κ-$(BEDT\text{-}TTF)_2X$ phases.[24,26] Overall the neutral molecules of the BEDT-TTF layer in the K and $NH_4$ salts describe an approximately hexagonal network, commensurate with that of the anion sublattice. The net effect is that the charged dimers are positioned in the neighborhood of the oxalate ions, leading to weak H-bonding between the terminal ethylene groups and oxalate O (2.51−3.05 Å). Short S···S distances are also observed between the molecules forming the dimers (3.46−

(21) Merrachi, E.-H.; Mentzen, B. F.; Chassagneux, F.; Boux, J. *Rev. Chim. Miner.* **1987**, *24*, 56−67.
(22) Wells, A. F. *Structural Inorganic Chemistry*, 4th ed.; Clarendon Press: Oxford, 1975; p 305.
(23) E.g.: Abdoud, K. A.; Clevenger, M. B.; de Oliveira, G. F.; Talham, D. R. *J. Chem. Soc., Chem. Commun.* **1993**, 1560−1562.
(24) E.g.: Yamochi, H.; Komatsu, T.; Matsukawa, N.; Saito, G.; Mori, T.; Kusunoki, M.; Sakaguchi, K. *J. Am. Chem. Soc.* **1993**, *115*, 11319−11327.
(25) Mori, T.; Inokuchi, H. *Bull. Chem. Soc. Jpn.* **1988**, *61*, 591−593.
(26) Kurmoo, M.; Pritchard, K. L.; Talham, D. R.; Day, P.; Stringer, A. M.; Howard, J. A. K. *Acta Crystallogr.* **1990**, *B46*, 348−354.

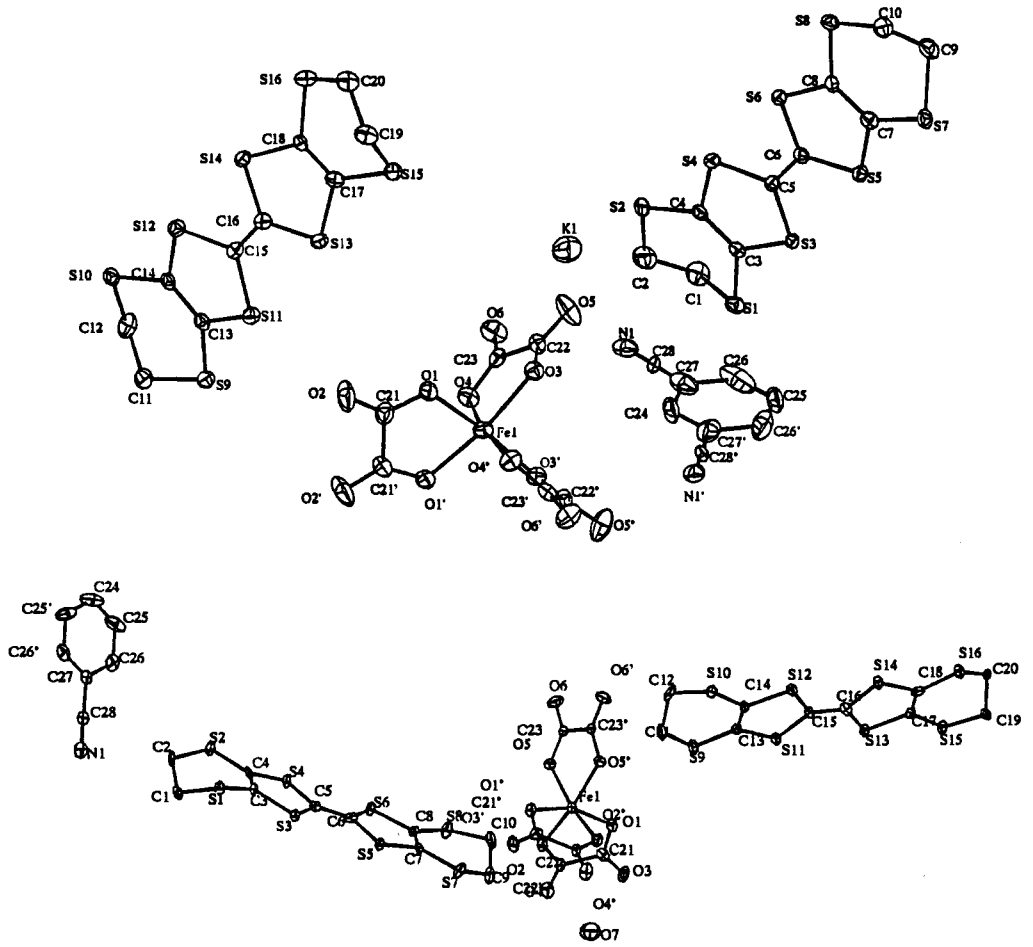

**Figure 1.** Atom numbering in (BEDT-TTF)$_4$AFe($C_2O_4$)$_3C_6H_5CN$ [A = K, $NH_4$ (a, top) and $H_2O$ (b, bottom)] including thermal ellipsoids.

3.77 Å) and likewise between the charged and neutral molecules (3.19−4.45 Å). Further evidence for specific interaction between the terminal $CH_2$ groups of the BEDT-TTF and the anion layer comes from the translation of the Fe($C_2O_4$)$_3^{3-}$ complexes within the plane of the anion layer on passing from one layer to the next. The displacement of the Fe($C_2O_4$)$_3^{3-}$ matches with the tilt of the long axes of the intervening BEDT-TTF. Thus the contacts between H atoms and O are the same at both ends of the BEDT-TTF.

Packing of the BEDT-TTF molecules in the $H_2O$ salt is quite different from that in the K and $NH_4$ salts: there are no discrete dimers (Figure 3b). Instead stacks are formed, with short S···S distances between them. Overall the packing closely resembles that of the $\beta''$-structure found in metallic (BEDT-TTF)$_2AuBr_2$[13] and the pressure-induced superconductor (BEDT-TTF)$_3Cl_2$·$2H_2O$.[27] Finally, the planes of the BEDT-TTF molecules in adjacent layers are twisted with respect to one another, an unusual feature in BEDT-TTF salts, the only other example known being one phase of (BEDT-TTF)$_2$Ag(CN)$_2$.[28]

**Electronic Band Structure.** The labeling of neighboring BEDT-TTF molecules in the A = K and A = $H_2O$ compounds are shown in Figure 4 and the respective band structures, electronic densities of states, and Fermi surface in Figure 5. The transfer integrals are listed in Table 4. As far as the semiconducting K salt is concerned, the very large value of the intradimer transfer integral (563 meV) is immediately apparent, five times bigger than any of the others (Figure 3a). This large value corresponds to a face-to-face (almost eclipsed) overlap of the two BEDT-TTF$^+$ molecules. In fact the transfer integrals between the undimerized BEDT-TTF which carry zero charge are ten times smaller (45−58 meV), while between the dimer and single molecules, several are zero, and only one (A − $\overline{\text{II}}$ (B) − b) has a substantial value (110 meV). It is important to recall that the magnitude of the intermolecular transfer integral depends on the directional character of the intermolecular overlap between S orbitals, as much as the S···S distances. The other BEDT-TTF compounds containing well-defined dimeric units are the superconducting $\kappa$-phase salts,[24,26] in which the intradimer transfer integrals lie within the range 200−300 meV, while all other integrals range between 50 and 150 meV. Moreover, the calculation shows that the difference in site energies between the crystallographically independent molecules, of the A = K salt (labeled A and B in Figure 4) amounts to 300 meV, while it is close to zero for the $\kappa$-(BEDT-TTF)$_2$Cu(NCS)$_2$ which contains two independent molecules of the same charge. However, in the present case this large difference and "dilution" of the dimers by individual BEDT-TTF serves to produce a closed shell semiconducting ground state, as indicated by the band structure shown in Figure 5a. The calculated band gap (0.3 eV) is in good agreement with that observed experimentally (0.28 eV). There exists certain similarity with the semiconducting salt $\kappa$-(MDT-TTF)$_2$Pt(CN)$_4$·$H_2O$[29] whose unit cell contains two orthogonal and independent dimers with different site energies and charges. One dimer exhibits an eclipsed geometry leading to a very large transfer integral, while the second intradimer integral is more than one-third smaller.

(27) Rosseinsky, M. J.; Kurmoo, M.; Talham, D. R.; Day, P.; Chasseau, D.; Watkin, D. *J. Chem. Soc., Chem. Commun.* **1988**, 88−90.

(28) Kurmoo, M.; Day, P.; Stringer, A. M.; Howard, J. A. K.; Ducasse, L.; Pratt, F. L.; Singleton, J.; Hayes, W. *J. Mater. Chem.* **1993**, *3*, 1161−1170.

(29) Ducasse, L.; Mousdis, G.; Fettouhi, M.; Ouahab, L.; Amiell, J.; Delhaes, P. *Synth. Met.* **1993**, *56/1*, 1995−2000.

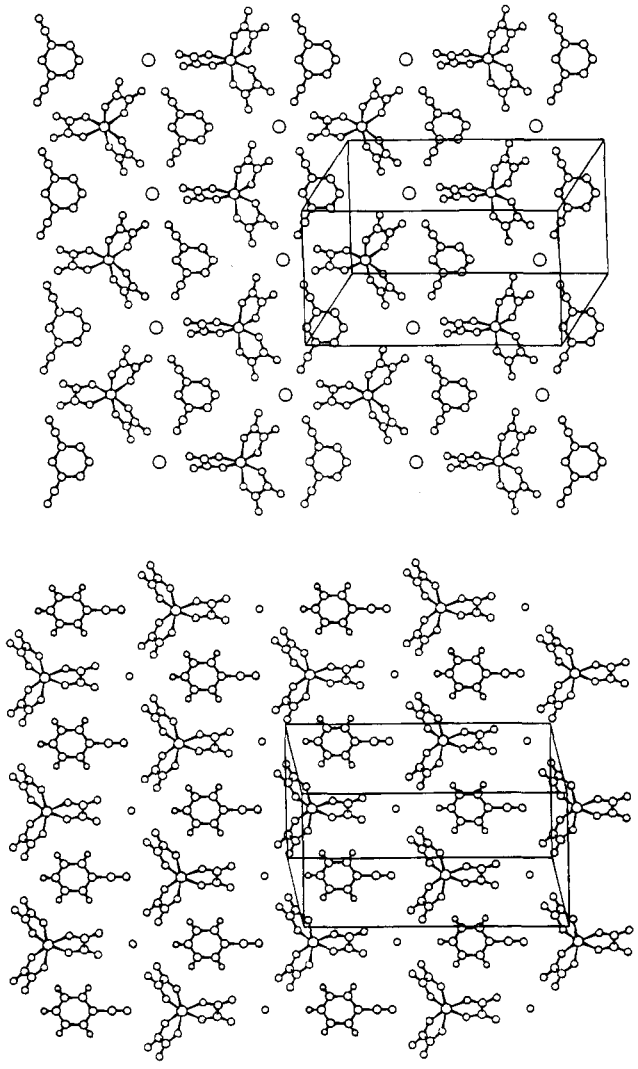

**Figure 2.** The anion and solvent layers in (BEDT-TTF)$_4$AFe($C_2O_4$)$_3$·$C_6H_5CN$: (a, top) A = K and (b, bottom) A = $H_2O$.

As in the present case, several transfer integrals are close to zero. The following sections indicate that the physical properties of the A = K salt agree with this prediction.

Turning to the A = $H_2O$ salt, we find the principal transfer integral values shown in Table 4. In contrast to the A = K salt no one transfer integral dominates the others though the largest (188 and 156 meV) are between molecules in the [110] direction. This is therefore expected to be the most highly conducting direction. Transfer integrals orthogonal to that direction are only slightly smaller, however (111 meV), so conduction within the layers should not be very anisotropic. The average charge on each BEDT-TTF is $+^3/_4$, so the conduction band is $^5/_8$ filled. The energy band structure (Figure 5b) indicates that the Fermi level intersects bands in the MX and MΓ directions, leading to a prediction of metallic behavior. In fact the band structure predicts the existence of electron and hole pockets in the Fermi surface, as shown in Figure 5c. The physical measurements described in the following sections show that this material is indeed a metal, and the bandwidth derived from the optical data (1.0 eV) is in good agreement with the calculated one (1.1 eV).

**Electrical Transport.** The K and $NH_4$ salts are both semiconductors over the temperature range 130−300 K with the same activation energy (0.14 eV) along all three crystal axes, though with markedly anisotropic conductivity.[30] The conductivity in two orthogonal directions within the basal plane is quite similar ($10^{-4}$ and 2 × $10^{-4}$ S cm$^{-1}$ at 300 K), and orthogonal

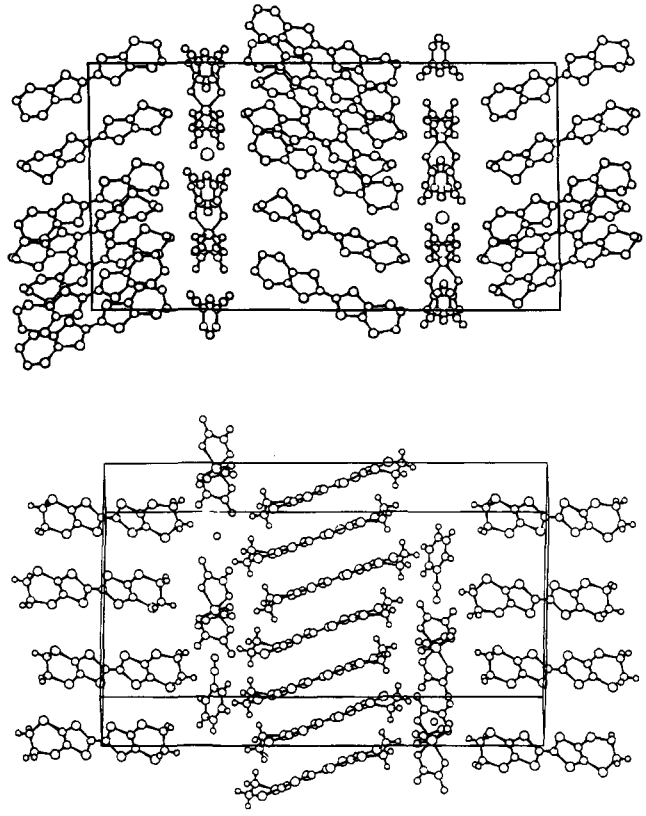

**Figure 3.** The layers of BEDT-TTF and anion layers in (BEDT-TTF)$_4$AFe($C_2O_4$)$_3$·$C_6H_5CN$: (a, top) A = K and (b, bottom) A = $H_2O$.

to the plane is 8 × $10^{-7}$ S cm$^{-1}$. In contrast the $H_2O$ salt is a metal with resistivity of ~$10^{-2}$ Ω cm at 200 K, decreasing monotonically by a factor of about 8 down to just below 7 K, at which temperature it becomes superconducting (Figure 6). In some crystals there is a small upturn in the resistance just above $T_c$, but in others it continues to diminish with decreasing temperature to the point where it falls suddenly to zero. The transition is sharp (width about 0.2 K), and there is very little hysterisis on cooling and warming within the resolution of the temperature controller (<0.1 K). Application of a magnetic field parallel to the long axis of the needle crystals broadens the transition toward lower temperature in the manner seen in other quasi-two-dimensional BEDT-TTF salts[31] so that the crystal remains resistive down to 2 K in fields above 0.7 T (Figure 7). With the applied field perpendicular to the needle axis the same effect is found at lower field (0.2 T) (Figure 8).

An important structural factor in the dimensionality of the conduction in the family of molecular charge transfer salts is the "thickness" of the anion layer separating the conducting planes of BEDT-TTF. A convenient measure of the thickness is the distance between the terminal C atoms of BEDT-TTF molecules on either side of the anion layer. Following that measure, a salt with a linear anion such as $Cu(NCS)_2^-$ has an effective thickness of 5.32 Å,[32] while ones with double anion layers like $[KHg(SCN)_4]^-$ are distinctly thicker (7.42 Å).[33] In the present compound the corresponding figure is 4.86 or 6.08

(30) Graham, A. W.; Kurmoo, M.; Day, P.; Coles, S. J.; Hursthouse, M. B.; Coomber, A. T.; Friend, R. H. *Mol. Cryst. Liq. Cryst.* In press.

(31) Ito, H.; Nogami, Y.; Ishiguro, T.; Komatsu, T.; Saito, G.; Hosoito, N. *Jpn. J. Appl. Phys.* **1992**, *7*, 419−425.

(32) Urayama, H.; Yamochi, H.; Saito, G.; Sato, S.; Kawamoto, A.; Tanaka, J.; Mori, T.; Maruyama, Y.; Inokuchi, H. *Chem. Lett.* **1988**, 463−466.

(33) Mori, H.; Tanaka, S.; Oshima, M.; Saito, G.; Mori, T.; Maruyama, Y.; Inokuchi, H. *Bull. Chem. Soc. Jpn.* **1990**, *63*, 2183−2190.

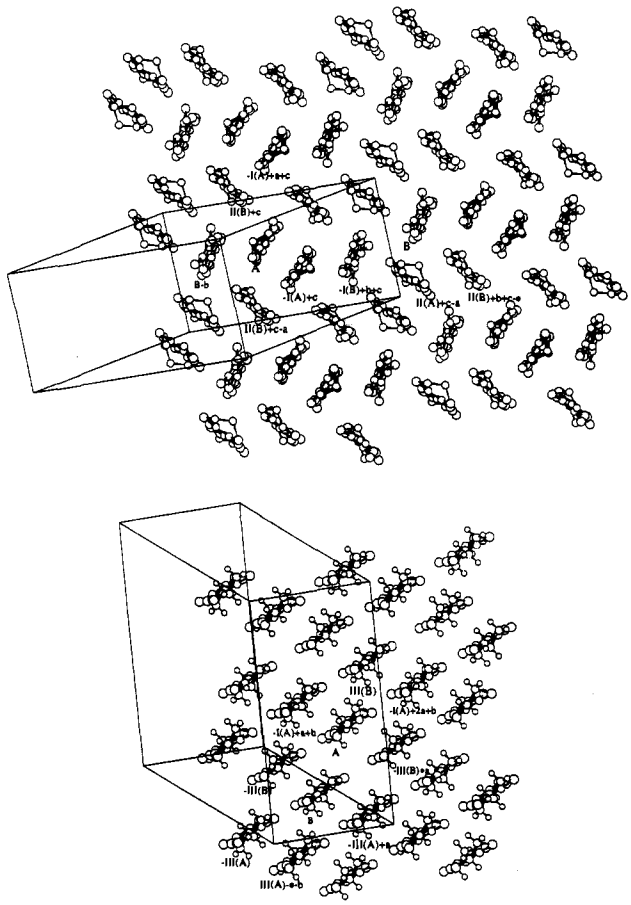

**Figure 4.** View of the BEDT-TTF layers along the C=C bonds including the labeling of neighboring BEDT-TTF molecules in (BEDT-TTF)$_4$AFe($C_2O_4$)$_3$·$C_6H_5CN$: (a, top) A = K and (b, bottom) A = $H_2O$.

Å depending on the BEDT-TTF molecule concerned. Evidently such a simple parameter cannot predict whether a given phase will be superconducting or not, or in case it is, what will be $T_c$, since the three cases quoted have $T_c$ 10.4, 1.1, and 7.0 K, respectively. Nevertheless it is interesting that the present compound has such a relatively high $T_c$.

**Magnetic Properties.** The bulk susceptibilities of polycrystalline samples of $(NH_4)_3Fe(C_2O_4)_3$·$3H_2O$ and (BEDT)$_4$AFe($C_2O_4$)$_3$·$C_6H_5CN$ (A = K, $H_2O$) were measured in a variety of field and temperature protocols to determine the contribution of the conduction electrons and those localized on the Fe to the total magnetic response. $(NH_4)_3Fe(C_2O_4)_3$·$3H_2O$ behaves as a Curie−Weiss paramagnet from 4−300 K with fitted $C$ = 4.38 emu K mol$^{-1}$ and $\Theta$ = −1.29 K. In the case of the semiconducting A = K compound the susceptibility can be fitted to the Curie−Weiss law over the entire temperature range from 2 to 300 K. The least-square fitted value of the Curie constant $C$ = 4.44 emu K mol$^{-1}$ and the Weiss constant = −0.25 K. On the assumption that $g$ = 2, and there is no orbital contribution to the moment the value of $C$ calculated for $S$ = $^5/_2$ is 4.375. Thus the Fe dominates the measured moment. In particular, there is effectively zero contribution from the BEDT-TTF, including those molecules whose bond lengths designate them as carrying a charge of +1. Hence the (BEDT-TTF)$_2^{2+}$ dimers are spin-paired, while the remaining BEDT-TTF contribute nothing to the paramagnetic susceptibility, in agreement with the assignment of zero charge.

The susceptibility of the superconducting A = $H_2O$ salt obeys the Curie−Weiss law from 300 to about 1 K above $T_c$, though in contrast to the semiconducting A = K salt, a temperature

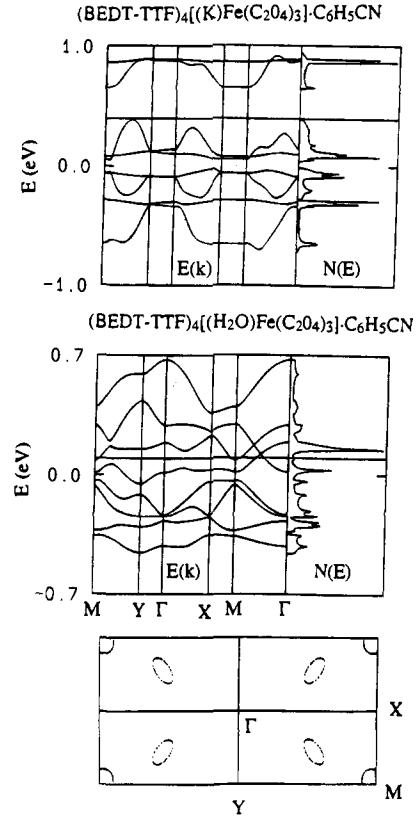


**Figure 5.** Band structures of (BEDT-TTF)$_4$AFe($C_2O_4$).$C_6H_5CN$: (a, top) A = K; (b, middle) A = $H_2O$; and (c, bottom) the calculated Fermi surface of (BEDT-TTF)$_4$($H_2O$)Fe($C_2O_4$)$_3$·$C_6H_5CN$ showing electron and hole (shaded) pockets.

**Table 4.** Transfer Integrals (meV) of (BEDT-TTF)$_4$AFe($C_2O4$)$_3$·$C_6H_5CN$ (A = K or $H_2O$)[a]

| | | | | | |
|---|---|---|---|---|---|
| | | A = K | | | |
| A | −I (A) + c | +563 | B | −I (B) + c + b | +45 |
| A | −II (B) − b | −110 | B | II(A) + c − a | 0 |
| A | −II (B) + c | 0 | B | II (A) + c | 0 |
| A | B − b | 0 | B | −II(A) | −106 |
| A | II (B) + c − a | 0 | B | II (B) + c + b | +58 |
| A | I + a + c | +11 | B | II (B) + c − a + b | +58 |
| −I (A) | II (B) + c − a | 0 | −II (B) | II (B) + c + b | +45 |
| | | A = $H_2O$ | | | |
| A | B | +156 | B | −III(B) | −46 |
| A | III (B) | +188 | B | III − a − b | 187 |
| A | −I (A) + a + b | −48 | B | −III (A) + a | −110 |
| A | −III (B) + a | −111 | B | III (A) | −92 |
| A | −I (A) + 2a + b | −109 | B | −III (B) + a | −58 |
| A | −III (B) | −92 | | | |

[a] The labeling of the molecules relates to Figure 4.

independent paramagnetic term is present amounting to 20 × $10^{-4}$ emu mol$^{-1}$. This may be compared with metallic compounds having varying numbers of holes in the conduction band, *viz.* 4 × $10^{-4}$ emu mol$^{-1}$ for one hole in $\beta$-(BEDT-TTF)$_2$-$AuI_2$[34] and 7 × $10^{-4}$ emu mol$^{-1}$ for two holes in (BEDT-TTF)$_3$-$Cl_2$·$2H_2O$.[35] The fitted Curie constant of 4.38 emu K mol$^{-1}$ is close to the value predicted for $Fe^{3+}$ ($^6A_1$), while the fitted $\Theta$ value (−0.2 K) signifies very weak antiferromagnetic exchange

(34) Talham, D. R.; Kurmoo, M.; Obertelli, D. S.; Parker, I. D.; Friend, R. H. *J. Phys. C.: Solid State Phys.* **1986**, *19*, L383−L388.
(35) Obertelli, S. D.; Marsden, I. R.; Friend, R. H.; Kurmoo, M.; Rosseinsky, M. J.; Day, P.; Pratt, F. L.; Hayes, W. In *Physics and Chemistry of Organic Superconductors*; Saito, G., Kagoshima, S., Eds.; Springer Proceedings in Physics 51; Springer-Verlag: Berlin, 1990; pp 181−184.
(36) Caulfield, J.; Blundell, S. J.; Du Croo de Jongh, M. S. L.; Hendriks, P. T. J.; Singleton, J.; Doporto, M.; House, A.; Perenboom, J. A. A. J.; Hayes, W.; Kurmoo, M.; Day, P. *Phys. Rev. B* **1995**, *51*, 8325−8336.

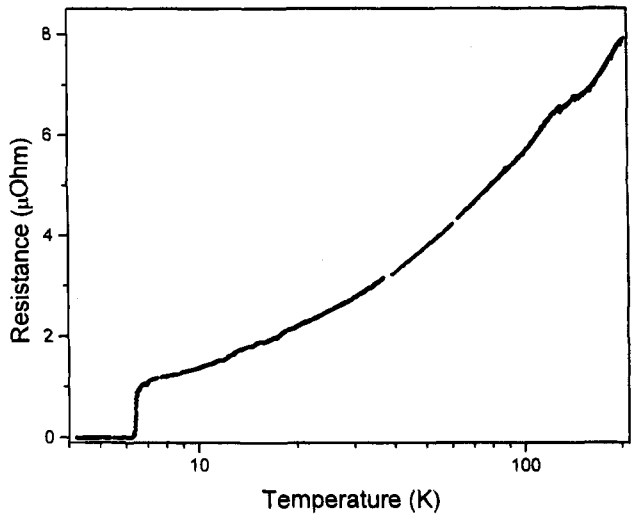


**Figure 6.** Temperature dependence of resistance of $(BEDT\text{-}TTF)_4(H_2O)Fe(C_2O_4)_3{\cdot}C_6H_5CN$ from 5–200 K.

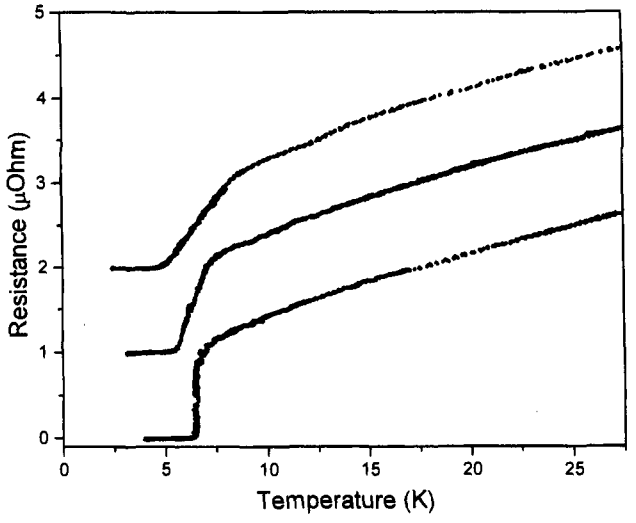


**Figure 7.** The superconducting transition in $(BEDT\text{-}TTF)_4(H_2O)Fe(C_2O_4)_3{\cdot}C_6H_5CN$ as a function of magnetic field applied parallel to the needle axis: H = 0; 0.2 T; 0.6 T (bottom to top; the plots are displaced by 1 $\mu$ohm).

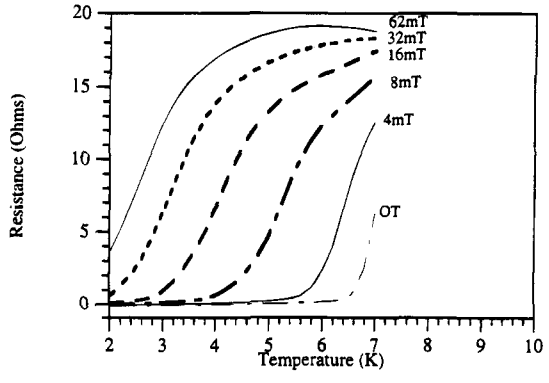


**Figure 8.** The superconducting transition as a function of magnetic field perpendicular to the needle axis from 0–62 mT.

between the Fe moments. As expected though, the temperature dependence of the susceptibility below 10 K is strongly dependent on the measurement field (Figure 9). When the sample is cooled to 2 K in zero field and then warmed in a measurement field of 0.5 mT, the susceptibility shows a distinct diamagnetic contribution expected in the superconducting temperature range, returning to Curie–Weiss behavior above

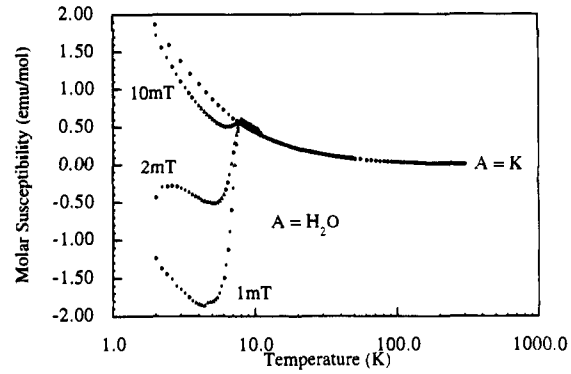


**Figure 9.** Temperature dependence of magnetic susceptibility of $(BEDT\text{-}TTF)_4AFe(C_2O_4)_3{\cdot}C_6H_5CN$: A = K (dots) and A = $H_2O$ (triangles).

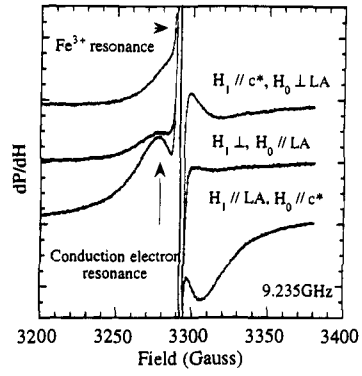


**Figure 10.** EPR spectra of $(BEDT\text{-}TTF)_4(H_2O)Fe(C_2O_4)_3{\cdot}C_6H_5CN$ at room temperature, at different crystal orientations.

10 K. On warming in increasingly large measurement fields the diamagnetic response diminishes, till it vanishes above 50 mT. At higher cooling or measurement fields (above 1 T) Curie–Weiss behavior persists down to 2 K, with a temperature independent contribution as at high temperature. Furthermore the onset of the diamagnetic contribution decreases from 8.0-(1) K (1 mT) to 7.2(2) K (40 mT). Finally the magnetization of both the $H_2O$ and K compounds at high field can be fitted quite precisely to a Brillouin curve for $S = {}^5/_2$, $g = 2$ with an extra contribution in the conductor for Pauli paramagnetism. To detect a Meissner effect the polycrystalline sample was cooled to 2 K in zero field, and the temperature dependence of the magnetization was measured in a field of 0.5 mT up to 20 K, followed by cooling in the same field. The Meissner effect is complete at 0.5 mT.

Further insight into the behavior of the magnetic electrons in both the semiconducting and superconducting compounds can be obtained from the EPR spectra of single crystals. The EPR spectrum of the semiconducting A = K compound consists of a single narrow resonance at $g = 2.002$ with peak to peak line width $H_{pp} = 1.6$ G independent of the crystal orientation. The line width and $g$-value are identical to those found in $K_3Fe(C_2O_4)_3{\cdot}3H_2O$ so the resonance is assigned to the $Fe^{3+}$. As expected, because of the closed shell structure of the BEDT-TTF no other resonance signal is observed. On the other hand, the room temperature EPR spectrum of the A = $H_2O$ compound consists of two resonances: an orientation independent narrow one ($H_{pp} = 1.5$ G) centered at 2.002, which can be assigned to the $Fe^{3+}$ by analogy with the A = K compound, and a much broader resonance ($g = 2.002–2.012$ and $H_{pp} = 23–35$ G) which we assign to the conduction electrons (Figure 10). The former peak is Lorentzian in shape at all orientations of the crystal, while the conduction electron resonance becomes Dysonian at certain orientations. Considering the small size of

the crystal this result points to a high conductivity, even at room temperature. Since the Dysonian line shape implies that the microwaves only penetrate the crystal to the skin depth, one would anticipate that all the resonances in the spectrum should have a similar line shape. It is therefore surprising that in the present case the $Fe^{3+}$ resonance remains Lorentzian, while that of the conduction electrons is Dysonian. As a tentative explanation, we suggest that the fact that the conducting BEDT-TTF layers and the "insulating" anion layers are of comparable thickness may permit transmission of the microwaves through the latter, at the same time reducing it through the former. Further work is needed to clarify this point.

The condition to observe separate resonances due to the simultaneous presence of localized and conduction electrons in a lattice is that a large difference exists between the respective $g$-values and relaxation rates of the two spin systems. In the present case one of these conditions is clearly met, because the $Fe^{3+}$ relaxation rate is high, producing a narrow signal. Furthermore, the loci of the two spin systems are certainly well separated spatially. Only in one other metallic charge transfer salt, (BEDT-TTF)$_3$$CuCl_4$·$H_2O$, have separated resonances due to conduction and 3d electrons been observed,[8] and there the angular dependence of the spectrum prevented direct comparison of the two line shapes. However in that compound, just as in the present example, the 3d ions are disposed in layers alternating with the BEDT-TTF sheets.

**Optical Reflectivity.** Figure 11 shows polarized spectra of the semiconducting (A = $NH_4$) and superconducting (A = $H_2O$) salts measured at room temperature. The spectrum of the semiconducting salt is less anisotropic than that of the metallic one and shows a broad electronic band which peaks near 2500 $cm^{-1}$ (0.3 eV). This result should be compared with the electrical conductivity measurement which also indicates a gap of 0.28 eV. The spectrum of the semiconducting salt also contains several sharp vibrational bands below 1700 $cm^{-1}$ which can be assigned to the oxalate C−O (1656 $cm^{-1}$ terminal and 1280 $cm^{-1}$ bridging) and C=C (1352 $cm^{-1}$) modes. When the electric vector is parallel to the layers, the spectrum of the metallic A = $H_2O$ salt is dominated by the electronic response with only weak vibrational structure superimposed, in contrast to the spectrum with electric vector perpendicular to the layers, which contains only vibrational bands. The Drude fit to the data observed in the parallel polarization is shown in Figure 11a. Analysis of the Drude edge was made using a one-dimensional model. The bandwidth is found to be 1.0 eV, in good agreement with that calculated for the band structure, and the optical mass (m*) is 1.0 $m_e$. This mass and the large enhancement of the magnetic susceptibility again emphasize the substantial correlation between carriers at the Fermi level.

## Conclusions

We have shown that the hexagonal layer motif $[AM^{III}(C_2O_4)_3]^{n-}$ containing bridging oxalate groups, which has been shown to form a wide variety of compounds with electronically inactive counter-cations having unusual cooperative magnetic properties[9], can also stabilize lattices containing the organic $\pi$-donor BEDT-TTF. In the compounds whose

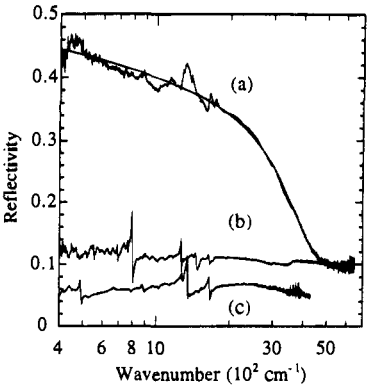


**Figure 11.** Room temperature polarized reflectivity spectra with the electric vector (a) parallel and (b) perpendicular to the layers of (BEDT-TTF)$_4$($H_2O$)Fe($C_2O_4$)$_3$·$C_6H_5CN$ and (c) parallel to the layers of (BEDT-TTF)$_4$($NH_4$)Fe($C_2O_4$)$_3$·$C_6H_5CN$.

structures we describe here, (BEDT-TTF)$_4$AFe($C_2O_4$)$_3$·$C_6H_5$-CN (A = $H_2O$, K, $NH_4$), the lattice is stabilized by $C_6H_5CN$ molecules included in the hexagonal cavities. The oxalato-bridged network of A and $M^{III}$ provides an elegant means of introducing transition metal ions carrying localized magnetic moments into the lattice of a molecular charge transfer salt. In the case of the A = $H_2O$ compound it has enabled us to prepare the first molecular superconductor containing localized magnetic moments within its structure, while the A = K, $NH_4$ compounds are semiconducting. The packing of the BEDT-TTF in the A = K, $NH_4$ phases is of a type not previously observed, with spin-paired $(BEDT\text{-}TTF)_2^{2+}$ separated by closed shell $(BEDT\text{-}TTF)^0$, while that in the superconductor is of $\beta''$ type. Both the superconducting A = $H_2O$ and semiconducting A = K, $NH_4$ phases contain high spin $3d^5$ $Fe^{III}$ with only very weak exchange interaction between them. Additional low temperature and high magnetic field experiments (e.g., of Schubnikov−de Haas oscillatory magnetoresistance[36]) will be needed to delineate the Fermi surface in the superconductor. A further synthetic challenge will be to incorporate other transition metal ions at the A site to create a two-dimensional magnetically ordered array between the BEDT-TTF layers. Our efforts are continuing in this direction.

**Acknowledgment.** We thank the UK Engineering and Physical Science Research Council and the European Union (DG XII) for financial support. We thank Drs. S. G. Carling and P. A. Pattenden for discussions and technical help.

**Supporting Information Available:** Tables of fractional atomic coordinates, isotropic and anisotropic displacement parameters, and bond lengths and angles (8 pages); listing of observed and calculated structure factors (20 pages). This material is contained in many libraries on microfiche, immediately follows this article in the microfilm version of the journal, can be ordered from the ACS, and can be downloaded from the Internet; see any current masthead page for ordering information and Internet access instructions.

JA952346T